Total dose test with γ-ray for silicon single photon avalanche diodes*

Qiaoli Liu(刘巧莉)[1,2], Haiyan Zhang(张海燕)[3], Lingxiang Hao(郝凌翔)[2], Anqi Hu(胡安琪)[2], Guang Wu(吴光)[3], and Xia Guo(郭霞)[2,†]

[1] *School of Information, Beijing University of Technology, Beijing* 100124, *China*

[2] *School of Electronic Engineering, State Key Laboratory for Information Photonics and Optical Communications, Beijing University of Posts and Telecommunications, Beijing* 100876, *China*

[3] *State Key Laboratory of Precision Spectroscopy, East China Normal University, Shanghai* 200062, *China*

(Received 15 February 2019; revised manuscript received 23 April 2020; accepted manuscript online 13 May 2020)

Gamma-ray (γ-ray) radiation for silicon single photon avalanche diodes (Si SPADs) is evaluated, with total dose of 100 krad(Si) and dose rate of 50 rad(Si)/s by using ^{60}Co as the γ-ray radiation source. The breakdown voltage, photocurrent, and gain have no obvious change after the radiation. However, both the leakage current and dark count rate increase by about one order of magnitude above the values before the radiation. Temperature-dependent current–voltage measurement results indicate that the traps caused by radiation function as generation and recombination centers. Both leakage current and dark count rate can be almost recovered after annealing at 200 °C for about 2 hours, which verifies the radiation damage mechanics.

Keywords: gamma-ray radiation, silicon single photon avalanche diode (Si SPAD), radiation damage

PACS: 85.30.De, 85.60.Dw, 85.60.Gz **DOI:** 10.1088/1674-1056/ab9286

1. Introduction

Single photon avalanche diodes (SPADs) are avalanche photodiodes (APD) operating in Geiger mode with bias higher than the breakdown voltage ($V_{\rm br}$). Due to the internal gain from avalanche effect, a single incident photon can trigger off a measurable current, which represents the ultimate sensitivity for a photodetector.[1,2] Silicon SPAD is one of the most qualified semiconductor photodetector by now for sensing a weak signal with wavelength ranging from 300 nm to 1100 nm due to its intact crystalline quality and large ratio of electron and hole ionization coefficients. Due to the advantages of ruggedness, compactness, suitability, and easiness to build integrated systems, Si SPADs are more competitive for the deep space applications.[3]

However, in the space environment, radiation may cause permanent performance degradation due to the energy deposition on the sensitive region of the device. The radiation dose rate is associated with obit and orbital inclination. It varies from 100 rad(Si)/year to 10 krad(Si)/year in low Earth orbit (LEO), 100 krad(Si)/year in medium Earth orbit (MEO), and over 10 krad(Si)/year in high Earth orbit (HEO).[4] Gamma-ray (γ-ray), which consists of the shortest wavelength electromagnetic waves and has a large penetration depth, is a kind of most energetic photons indicating highly destructive power.[5,6] In the case of γ-ray radiation, taking ^{60}Co γ-ray source as an example, the radiation effect is mainly through Compton scattering.[3] It mainly causes electron ionization and atomic displacement.[7,8] The former can generate positive charges and oxide trapped charges, as well as interface traps at the SiO_2/Si interface, which act as generation centers for a surface current if exposed to an electric field.[9] The displacement damage is mainly through Compton scattering by the photon with energy far greater than the binding energy of the atomic electrons.[10] The energetic Compton electron interacts with the Si lattice, and then Si atoms in the bulk material will be displaced from their host lattice positions and defects will be generated if the energy from the scattered electrons is high enough. Defects in the device play an important role for the increase of the leakage current and DCR, and then the reduction of the sensitivity. Hence, it is mandatory to assess the performance of a SPAD after exposed in the γ-ray radiation environment.

This paper reports the results of γ-ray radiation hardness test for Si SPADs with a total dose of 100 krad(Si) and a dose rate of 50 rad(Si)/s by using ^{60}Co as the radiation source. The purpose of this experiment is to assess the laser time transfer payloads equipped on the BeiDou navigation satellite system. It is found that the $V_{\rm br}$, photocurrent, and gain have no measurable changes after radiation. However, both leakage current and DCR of the device after radiation increase by about one order of magnitude. The carrier transport dynamics after radiation, which is verified by the annealing experiment, is analyzed by the temperature-dependent current–voltage (I–V) measurement.

2. Experiments

An epitaxial-based planar n^+–p–p^-–p^+ SPAD structure with a diameter of 200 μm in this work is fabricated by complementary metal oxide semiconductor (CMOS) technology.

*Project supported by the National Key Research and Development Program of China (Grant No. 2017YFF0104801).

†Corresponding author. E-mail: guox@bupt.edu.cn

Si epitaxial is grown on the heavily-doped p^+-Si substrate with ⟨111⟩ crystallographic orientation. The p-type multiplication layer is then formed by implantation method, followed by annealing process. The guard ring, p^+ stopper ring, and n^+ ohmic contact layer are also formed by ion implantation. The active region is surrounded by the p^+ stopper ring at the edge of the chip which stops space charge at the SiO_2/Si interface. An optimized SiO_2 antireflecting coating is applied to increase the light incident efficiency. Finally, the chips are all sealed in a standard TO-46 case with a glass window on the frontside.

The radiation test of the Si SPADs has been conducted at room temperature with γ-rays, which were produced by a ^{60}Co source. The SPAD chips under test were sealed in a standard TO-46 case with a glass window on the frontside. Then they were exposed to the ^{60}Co γ-ray source directly with a distance about 3 cm to ensure the dose rate of 50 rad(Si)/s. The total dose was 100 krad(Si). The SPADs were divided into three groups with different bias conditions (unbiased, 0.9 V_{br}, 1.1 V_{br}) during the radiation test. The leakage current was measured both before and after radiation (within three hours) using Keithley 6517B Elctrometer. A tungsten-halogen lamp (Zolix LSH-T75) and a grating monochromator (Zolix Omni-λ3005) were employed in the measurement of the photocurrent under the wavelength of 532 nm. The SPAD was operated in passive-quenching Geiger mode, while the bias voltage on the SPAD was higher than V_{br}. The avalanche pulse would be triggered and discriminated, while photons or dark noise occurred. Then the avalanche would be quenched by the large resistor. The DCR was recorded by an oscilloscope (Iwatsu SS7840H).

3. Results

The photocurrent and gain of the devices show negligible changes after radiation. Figure 1(a) shows the photocurrent and corresponding gain results under the incident wavelength of 532 nm, the sample biased at 1.1 V_{br} under radiation is taken for example. The slight rising of leakage current could not make obvious change of the photocurrent and gain. From the electrical measurement, the negligible change of V_{br}, which is about 33 V, has been observed for all the samples in the inset of Fig. 1(b), indicating that the doping level of the whole structure has not been remarkably changed by the defects caused by the γ-ray radiation. However, the leakage current is really affected by the γ-ray radiation, as shown in Fig. 1(b). Compared with the value before radiation, the leakage current still remains at a low level of about 10^{-10} A. The increase of the leakage current is around one order of magnitude for all the devices under test. As shown in Table 1, the leakage current at 29.7 V is 351 pA, 667 pA, and 151 pA, respectively, for the devices under the biases of 0.9 V_{br} (29.7 V), 1.1 V_{br} (36.3 V), and unbiased during the radiation test. It can be seen that the degradation degree of leakage current becomes severe with increasing bias during the radiation test. Table 2 shows the radiation effect on the DCR performance, which is measured by keeping PDE at about 5% under the wavelength of 532 nm. DCR of the devices before radiation is about 300 cps/μm^2, where cps is short for counts per second. Correspondingly, DCR also increases by about one order of magnitude after the radiation, and also strongly depends on the bias condition during the γ-ray exposure.

Table 1. Leakage current changes at 29.7 V before and after γ-ray radiation test.

Condition	Leakage current
before radiation	28 pA
unbiased	151 pA
0.9 V_{br}	351 pA
1.1 V_{br}	667 pA

Table 2. Comparison of DCR before and after radiation while keeping PDE at 5%.

Condition	DCR
before radiation	300 cps/μm^2
0.9 V_{br}	5.1×10^3 cps/μm^2
1.1 V_{br}	11.5×10^3 cps/μm^2

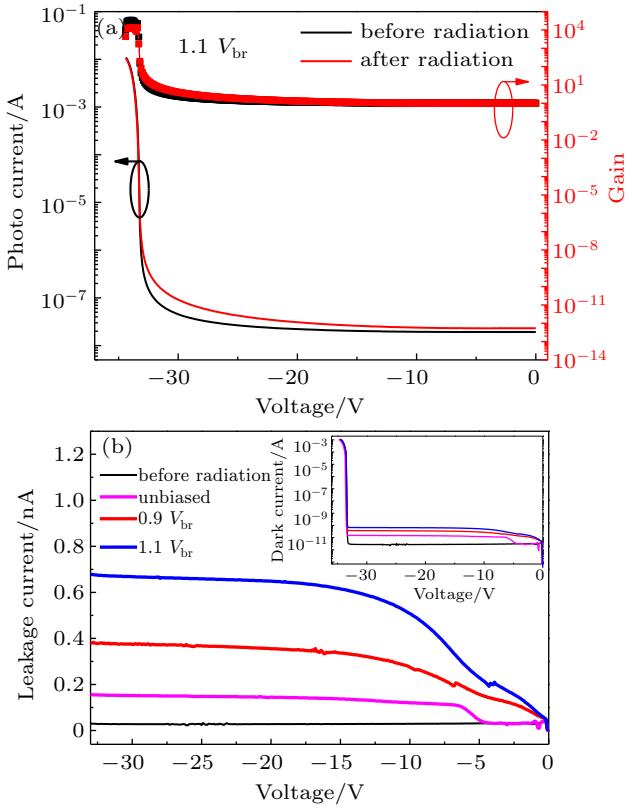

Fig. 1. (a) The measured photocurrent and corresponding gain at 532 nm of the devices biased at 1.1 V_{br}, which show negligible variations compared with the values before radiation. (b) Leakage current as a function of reverse voltage before and after radiation at room temperature. During the radiation, the samples are biased at 0.9 V_{br}, 1.1 V_{br} and unbiased, respectively, with the total radiation dose of 100 krad(Si) and dose rate of 50 rad(Si)/s. The inset shows the negligible changes of V_{br} after radiation.

To further gain the effect of radiation on carrier transport dynamics, the temperature-dependent forward and reverse I–V characteristics are investigated from 60 K to 300 K before

and after radiation, respectively. The Arrhenius plots of the forward and reverse *I*–*V* curves after radiation are shown in Figs. 2(a) and 2(b), respectively. $V_{\rm br}$ decreases as the temperature decreases from 300 K to 60 K, with a positive temperature coefficient (0.02 V/K), indicating a true avalanche breakdown occurred.[11] According to the forward current equation

$$I_{\rm F} = I_0 \exp\left(\frac{qV}{nkT}\right), \tag{1}$$

where $I_{\rm F}$, I_0, q, V, n, k, and T are the forward current, saturation current, electron charge, voltage bias, ideality factor, Boltzmann constant, and temperature, respectively. The ideality factor n at different temperature can be extracted and plotted in Fig. 2(c). It decreases with temperature from 5.8 at 60 K to 1.8 at 300 K after the radiation, whereas decreases with temperature from 5.9 to 1.2 before the radiation. Generally, the current is mainly composed of diffusion and recombination currents when n is between 1 and 2 (210 K to 300 K).[12] When n is larger than 2 ($<$ 210 K), the tunneling mechanism should be dominant.[13] Compared with the ideality factor before radiation, the discrepancy at the same temperature increases from 0.1 at 60 K to 0.6 at 300 K, which indicates the generation of new recombination generation centers at the interface and/or in the depletion region caused by the γ-ray radiation.[14]

The ideality factor fits the model of tunneling enhanced interface recombination very well at lower temperature ($<$ 210 K), which is given by the following equation:

$$n = \frac{E_{00}}{kT} \coth\left(\frac{E_{00}}{kT}\right), \tag{2}$$

where E_{00} is the characteristic tunneling energy, showing the contribution of tunneling to the recombination process.[15] According to the fitting results in Fig. 2(c), E_{00} is changed from 29 meV to 31 meV for the device after the radiation. The little change of E_{00} implies that the amount of interface traps is not greatly increased, and the interface traps are not the dominant factor.

Figure 2(d) depicts the Arrhenius plot of leakage current at 20 V as a function of temperature before and after radiation, respectively. According to the reverse current ($I_{\rm R}$) equation

$$I_{\rm R} \propto \exp(-E_{\rm a}/kT), \tag{3}$$

the activation energy $E_{\rm a}$ is 0.12 eV and 0.56 eV before and after radiation, respectively.[16] $E_{\rm a}$ derived before the radiation is much less than half of the bandgap of Si, which is consistent with the weak temperature dependence of the tunneling current.[17] After the radiation, $E_{\rm a}$ approaches half of the energy bandgap of Si, implying that the generation recombination current from the depletion region composes the main leakage current, mainly from the defects or traps caused in the bulk.[18] This is also the reason for the increase of DCR, due to the increase of carriers generated by trap-assisted thermal generation and trap-assisted tunneling, which are the main origins of DCR.[19]

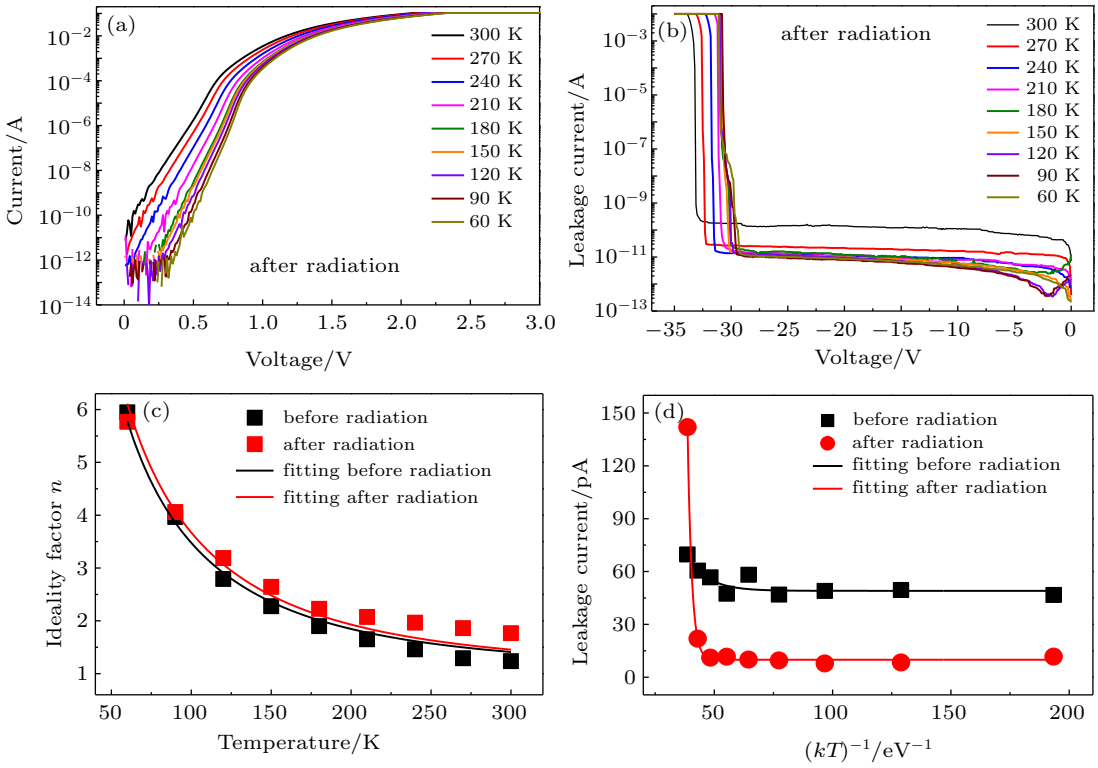

Fig. 2. Temperature-dependent (a) forward and (b) reverse *I*–*V* curves. (c) Comparison of measured temperature-dependent ideality factor n and their fitting results before and after radiation. (d) Arrhenius plot of leakage current measured at 20 V and the fitting results as a function of temperature before and after radiation.

In order to verify the radiation effect on the Si SPAD chips, annealing experiment was carried out. Figure 3 monitors the leakage current of a Si SPAD after radiation at room temperature without bias. As shown by the red squares, it increases at first 300 hours from 50 pA to 151 pA firstly, which is owing to the increased density of interface traps, whose long build-up time is determined by the transport of a positively charged ion, probably H^+, through the oxide.[20] The decrease of the leakage current in the following 268 hours may be due to the recovery of vacancy-interstitial pairs nearby. However, the leakage current is still as high as 40 pA due to the existing oxide trapped charges and interface traps, and also traps inside the avalanche junction. After annealing at 200 °C for 2 hours, an obvious reduction of the leakage current is observed. The leakage current (14 pA) approaches its initial value before radiation (black square). Correspondingly, DCR also decreases to 1.3×10^3 cps/μm^2 at 33 V after annealing at 200 °C. During this process, hole de-trapping may occur by thermal emission of holes from the traps in the oxide or hop to the interface and into silicon.[21] Besides, the originally displaced atoms caused by Compton scattering could gain enough energy to move back to their host lattice positions, which results in the reduction of the traps or defects. The reduction of the trap number both in the bulk and interface is determined by the temperature and time. The recovery of the noise level of the weakened device by annealing and the anti-radiation performance reach the space availability.

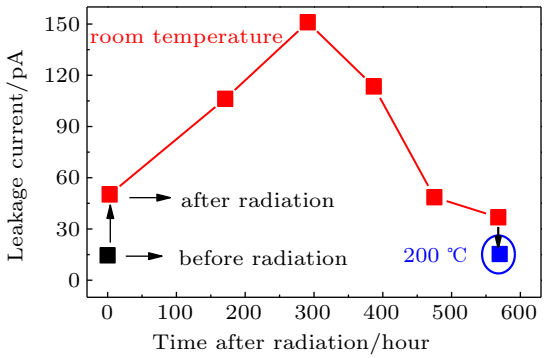

Fig. 3. Time evolution of leakage current after radiation. Leakage current of the unbiased device is traced at 29.7 V at room temperature for 568 hours (red square) and annealed at 200 °C for 2 hours (blue square), after which the leakage current approaches its initial value before radiation (black square).

4. Conclusion

Total dose test results with γ-ray for silicon SPADs are presented. The breakdown voltage, photocurrent, and gain demonstrate their stability even after exposure to γ-rays, which guarantees a stable operation of Si SPADs. While the leakage current and DCR increase by about one order of magnitude compared with the values before radiation. Temperature-dependent I–V measurement results reveal the trap-assisted generation carrier transport dynamics inside the device. The leakage current and DCR can be almost recovered after annealing at 200 °C for about 2 hours, which further verifies the radiation damage effect on the devices. The recovery of the original noise level after annealing indicates a reasonable method to fulfill its space application.

Acknowledgment

All the authors thank Mr. G. X. Cao and Mrs. C. Li of China Academy of Space Technology for useful discussion.

References

[1] Dautet H, Deschamps P, Dion B, MacGregor A D, MacSween D, McIntyre R J, Trottier C and Webb P P 1993 *Appl. Optics* **32** 3894
[2] Vines P, Kuzmenko K, Kirdoda J, Dumas D C, Mirza M M, Millar R W, Paul D J and Buller G S 2019 *Nat. Commun.* **10** 1
[3] Pagano R, Lombardo S, Palumbo F, Sanfilippo D, Valvo G, Fallica G and Libertino S 2014 *Nucl. Instrum. Methods A* **767** 347
[4] Manning R 1993 *16th Annual AAS Guidance and Control Conference* **93** 179
[5] Dixit V K, Khamari S K, Manwani S, Porwal S, Alexander K, Sharma T K, Kher S and Oak M 2015 *Nucl. Instrum. Methods A* **785** 93
[6] Pagano R, Lombardo S, Palumbo F, Sanfilippo D, Valvo G, Fallica G and Libertino S 2014 *Nucl. Instrum. Methods A* **767** 347
[7] Irani K H, Pil-Ali A and Karami M A 2017 *Opt. Quant. Electron.* **49** 292
[8] Moscatelli F, Marisaldi M, Maccagnani P, Labanti C, Fuschino F, Prest M, Berra A, Bolognini D, Ghioni M, Rech I, Gulinatti A, Giudice A, Simmerle G, Candelori A, Mattiazzo S, Sun X, Cavanaugh J F and Rubini D 2013 *Nucl. Instrum. Methods A* **711** 65
[9] Goiffon V, Cervantes P, Virmontois C, Corbière F, Magnan P and Estribeau M 2011 *IEEE T. Nucl. Sci.* **58** 3076
[10] Gill K, Hall G and MacEvoy B 1997 *J. Appl. Phys.* **82** 126
[11] Chynoweth A G and McKay K G 1957 *Phys. Rev.* **106** 418
[12] Dalapati P, Manik N B and Basu A N 2014 *Cryogenics* **65** 10
[13] Yan D, Lu H, Chen D, Zhang R and Zheng Y 2010 *Appl. Phys. Lett.* **96** 083504
[14] Dalapati P, Manik N B and Basu A N 2014 *J. Semicond.* **35** 082001
[15] Nadenau V, Rau U, Jasenek A and Schock H W 2000 *J. Appl. Phys.* **87** 584
[16] Pattabi M, Krishnan S and Sanjeev G 2007 *Sol. Energ. Mat. Sol. C* **91** 1521
[17] Feng Y J, Li C, Liu Q L, Wang H Q, Hu A Q, He X Y and Guo X 2018 *Chin. Phys. B* **27** 048501
[18] Yang S, Zhou D, Cai X, Xu W, Lu H, Chen D, Ren F, Zhang R and Zheng Y 2017 *IEEE T. Electron Dev.* **64** 4532
[19] Cheng Z, Zheng X, Palubiak D, Jamal Deen M and Peng H 2016 *IEEE Tran. Electron Dev.* **63** 1940
[20] Saks N S, Dozier C M and Brown D B 1988 *IEEE Tran. Nucl. Sci.* **35** 1168
[21] McWhorter P J, Miller S L and Miller W M 1990 *IEEE Tran. Nucl. Sci.* **37** 1682